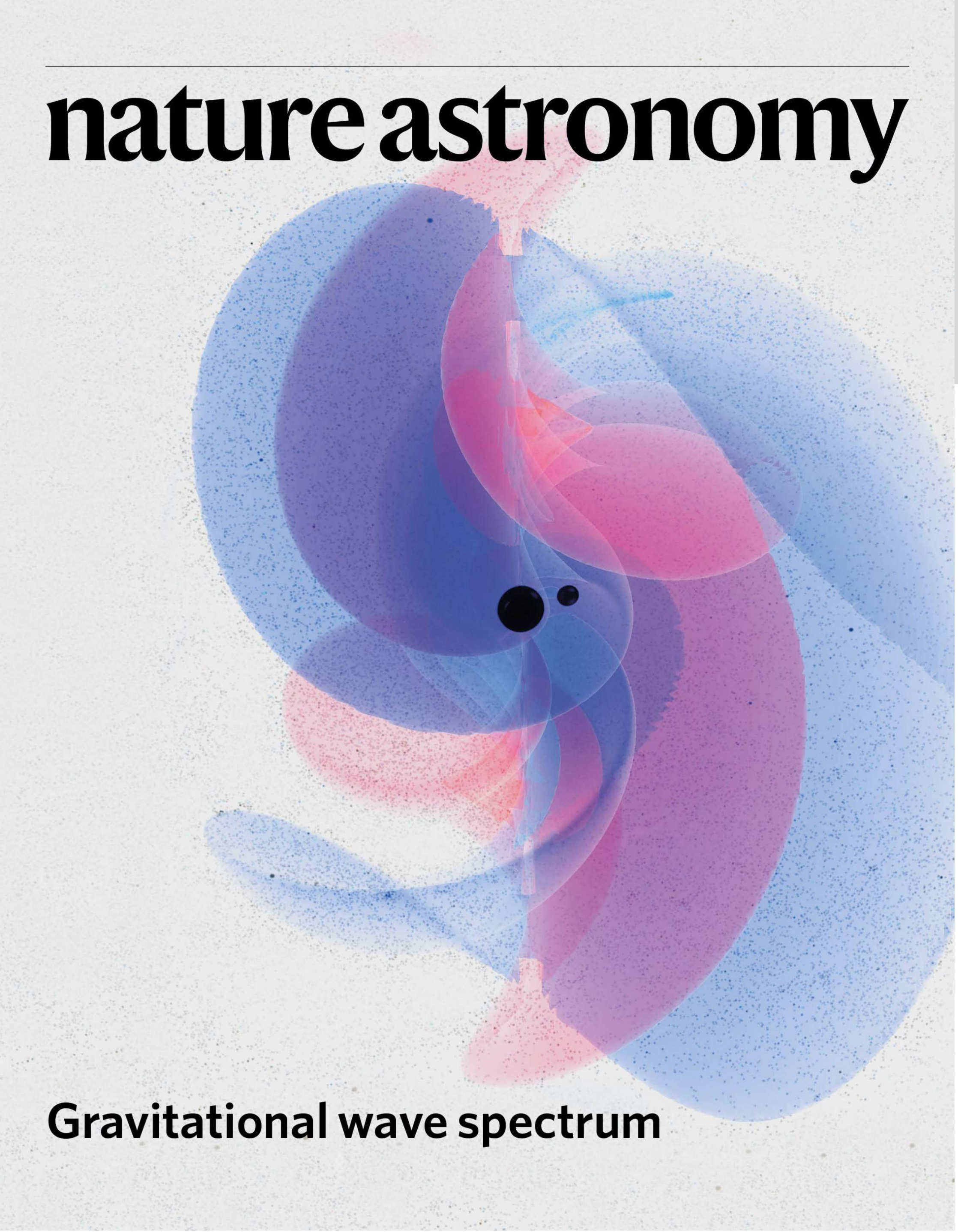

Spinning binary black hole mergers in galactic GC's and gravitational wave signals

Margarita Sobolenko
MAO NASU, Kyiv, Ukraine

Collaborators:
Peter Berczik
Manuel Arca Sedda
Miroslaw Giersz
Konrad Maliszewski
Oleksandr Veles

Volkswagen Trilateral Project Dynamical Mechanisms of Accretion in Galactic Nuclei

Sep. 6-8, 2021

Detectability of intermediate-mass black holes in multiband gravitational wave astronomy
Karan Jani, Deirdre Shoemaker &
Curt Cutler
Volume 4 Issue 3, March 2020

LIGO-Virgo: O1 and O2 events 2015-2017

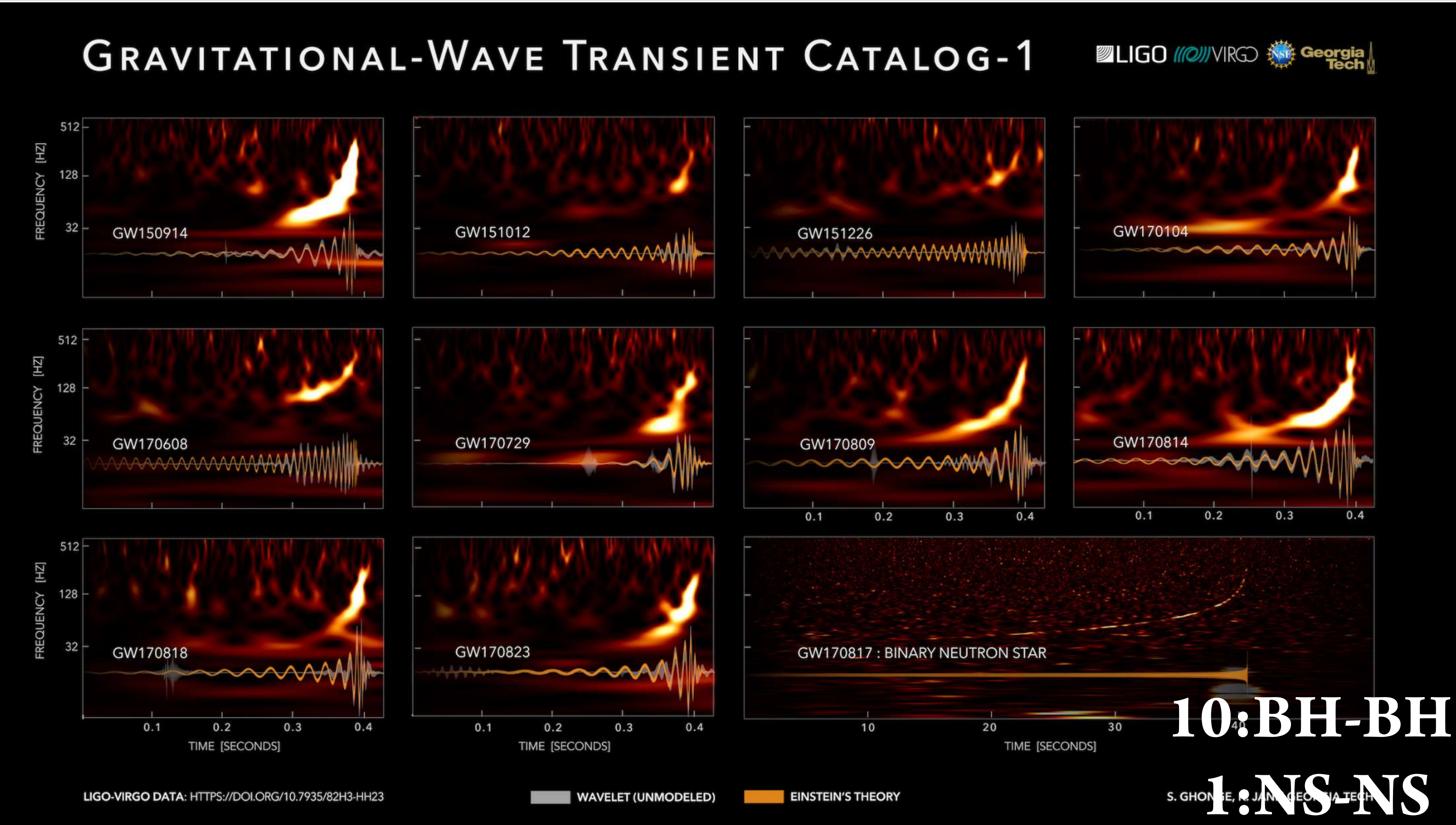

GWTC-1: A Gravitational-Wave Transient Catalog of Compact Binary Mergers Observed by LIGO and Virgo during the First and Second Observing Runs

***Phys. Rev. X* 9, 031040** – Published 4 September 2019

LIGO-Virgo: O3a events 04/2019-09/2019

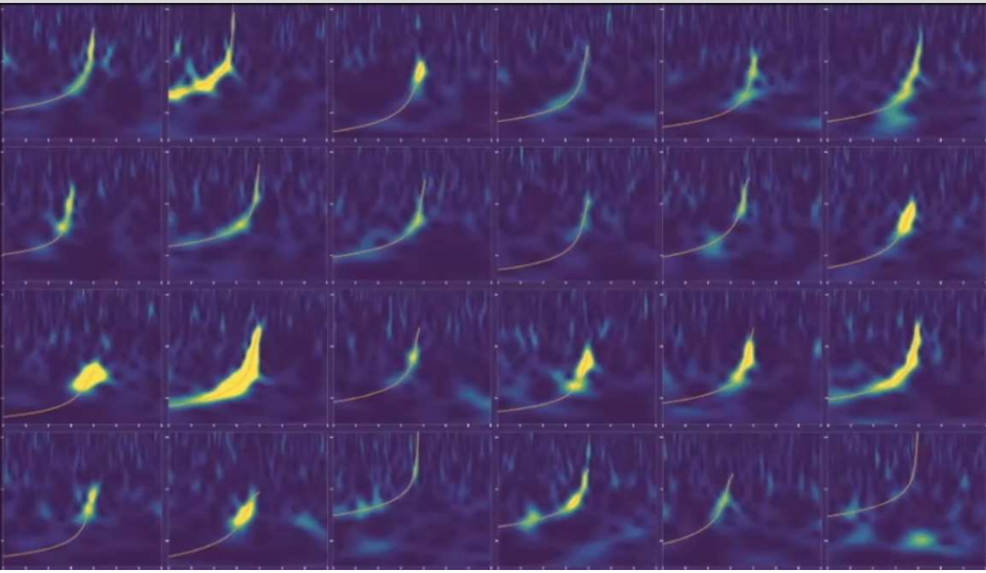

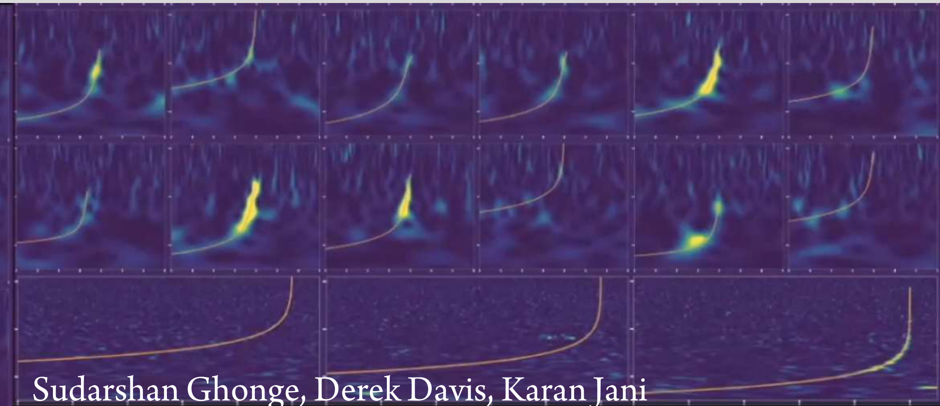

GWTC-2.1: Deep Extended Catalog of Compact Binary Coalescences Observed by LIGO and Virgo During the First Half of the Third Observing Run
arXiv:2108.01045
Published 2 August 2021

GWTC-2: Compact Binary Coalescences Observed by LIGO and Virgo during the First Half of the Third Observing Run
Phys. Rev. X 11, 021053
Published 9 June 2021

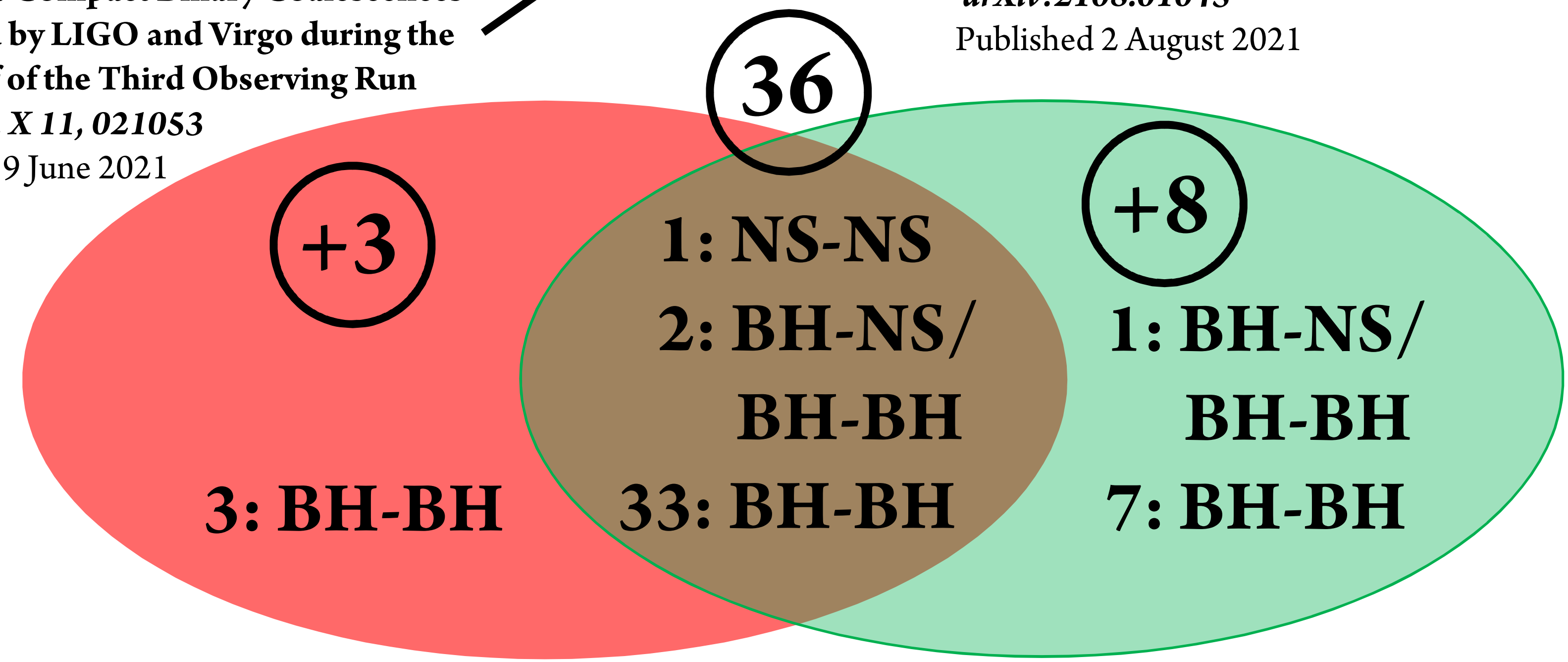

Black hole spin

- **Total angular momentum** of the binary:

$$\boldsymbol{J} = \boldsymbol{L} + \boldsymbol{S_1} + \boldsymbol{S_2},$$

where $\boldsymbol{L}$ is orbital angular momentum and $\boldsymbol{S_{1,2}}$ is individual BHs spin.

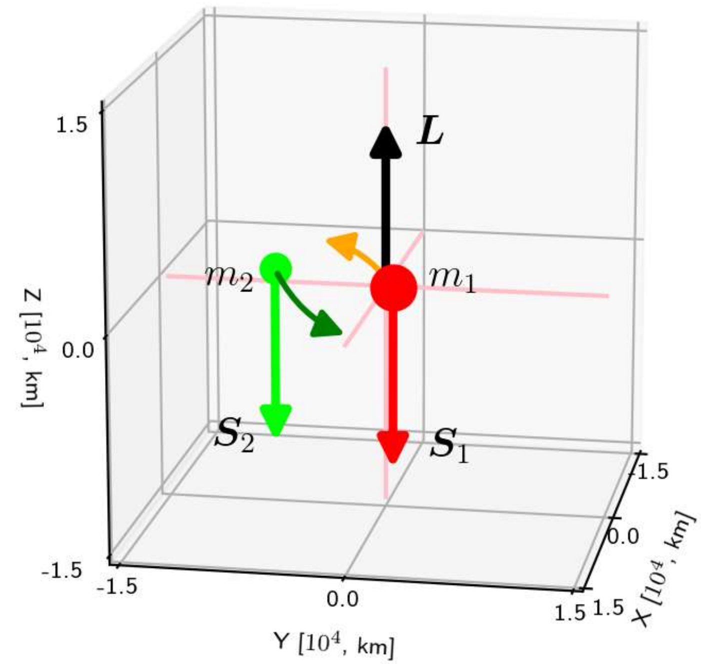

- **Spin** can be written:

$$\left|\boldsymbol{S_{1,2}}\right| = \chi_{1,2} \frac{G m_{1,2}^2}{c},$$

where $\chi_{1,2} \in [0,1]$ is **dimensionless spin magnitude**. Dimensionless spin magnitude was limited by values 0, 1 or -1 independently for two BHs in three directions *x, y, z*. Total number of spin combinations is 49.

- **Post-Newtonian** terms were taken up to 3.5PN + spin-orbit terms + spin-spin terms:

$$\frac{d\mathbf{v}}{dt} = \mathbf{a}_{\mathrm{N}} + \frac{1}{c^2}\mathbf{a}_{1\mathrm{PN}} + \frac{1}{c^2}\mathbf{a}_{1.5\mathrm{PN,SO}} + \frac{1}{c^4}\mathbf{a}_{2\mathrm{PN}} + \frac{1}{c^4}\mathbf{a}_{2\mathrm{PN,SS}} + \\ + \frac{1}{c^5}\mathbf{a}_{2.5\mathrm{PN}} + \frac{1}{c^4}\mathbf{a}_{2.5\mathrm{PN,SO}} + \frac{1}{c^6}\mathbf{a}_{3\mathrm{PN}} + \frac{1}{c^7}\mathbf{a}_{3.5\mathrm{PN}} + O\left(\frac{1}{c^8}\right)$$

- **Gravitational wave strain**:

$$h^{ij} \approx \frac{4G\mu}{Dc^4}\left[v^i v^j - \frac{Gm}{r} n^i n^j\right] \longrightarrow \begin{matrix} h_+ \\ h_\times \end{matrix} \text{ polarization}$$

Black hole spin in LIGO-Virgo-KAGRA

- **Effective inspiral spin parameter** (***Damour 2001PhRvD.64l4013D***) measures the mass-averaged spin along the orbital angular momentum axis, that LIGO can infer from the gravitational waveform:

$$\chi_{\rm eff} = \frac{m_1\chi_1 \cos\theta_1 + m_2\chi_2 \cos\theta_2}{m_1+m_2}.$$

$\chi_{\rm eff} = 1$: $\boldsymbol{S}\uparrow\uparrow\boldsymbol{L}$ $\chi_{\rm eff} = 0$: $\boldsymbol{S_1}\downarrow\uparrow\boldsymbol{S_2}$

$\chi_{\rm eff} = -1$: $\boldsymbol{S}\downarrow\downarrow\boldsymbol{L}$ $\chi_{1,2} \ll 0$

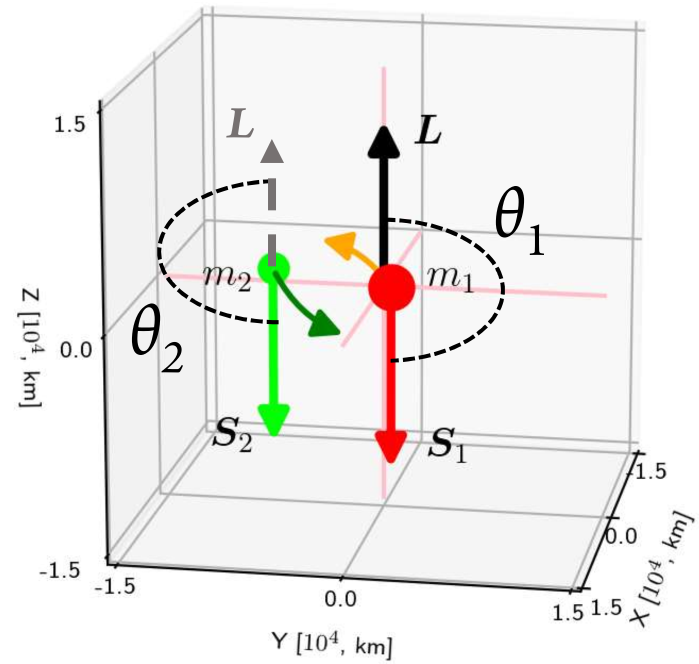

- The effective **precessing spin** (***Schmidt et al. 2015PhRvD.91.024043***) measures the spin in the orbital plane, perpendicular to orbital angular momentum axis:

$$\chi_{\rm p} \sim \chi_1 \sin\theta_1.$$

- In a post-Newtonian expansion, the evolution of the waveform's phase depends only on **chirp mass** (***Cutler & Flanagan 1994PhRvD.49.258C***):

$$\mathcal{M} \equiv (m_0 m_1)^{3/5}(m_0+m_1)^{-1/5},$$

where ***mass ratio*** $q = m_1/m_0$ ($m_1 < m_0$) and total mass $M = m_1 + m_0$.

Set of models I (SI): Initial parameters

Breaching the limit: formation of GW190521-like and IMBH mergers in young massive clusters

Manuel Arca Sedda,[1] Francesco Paolo Rizzuto,[2] Thorsten Naab,[2] Jeremiah Ostriker,[3,4] Mirek Giersz,[5] and Rainer Spurzem[1,6,7]

arXiv:2105.07003 (ApJ accepted)

Simulation ID	Merger generation	σ_{YC} km s^{-1}	M_a $M_\odot$	M_b $M_\odot$	q	sma $R_\odot$	e
IMBH-BH mergers							
R06W9sim3	Gen-1	7	328	21	0.064	1.21	0.41
R06W9sim7	Gen-1	6	307	22	0.072	0.7	0.085
R06W9sim7	Gen-2	6	329	26	0.079	697	0.997
R06W6sim6	Gen-1	10	285	22	0.077	36.7	0.955

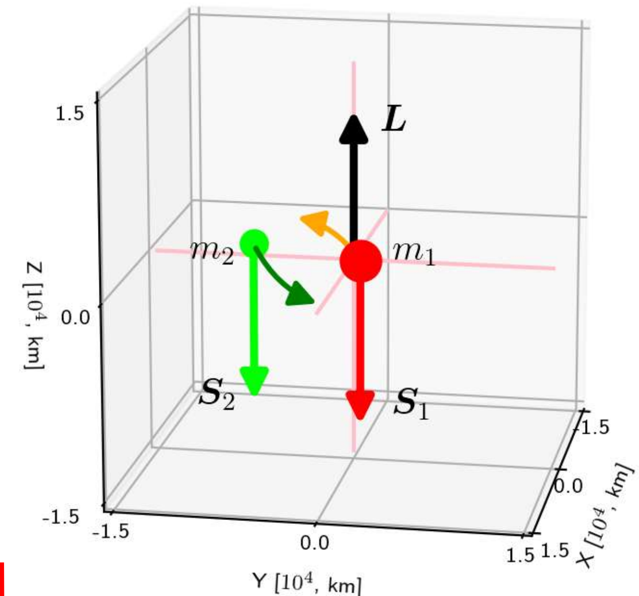

Peters & Mathews 1963PhRv, 131, 435
Peters 1964PhRv, 136, 1224
Peters 1964PhDT

Just 2.5*PN*

Simulation ID	Merger generation	t_{form} Myr	t_{gw} yr	(5.6) $t_{gw} = -\frac{a}{da/dt}$ yr	(5.9+5.10) circ. orbit yr	last eq. near 1 yr	(5.6+5.7) rk4 yr	sim. up to 3.5$\mathcal{PN}$ yr
R06W9sim3	Gen-1	113	44	185	134	127	70	69
R06W9sim7	Gen-1	348	16	62	16	29	16	16
R06W9sim7	Gen-2	369	3e4	1.8e5	1.2e13	3.5e5	4.5e5	4.10948e5
R06W6sim6	Gen-1	11.2	8.5e3	2.8e4	1.4e8	5.2e4	3.8e4	4.1326e4

4 (3 long runs with reduced Δt_{out}) + 4*49 spin runs = **200 models**

SI: waveforms for $h_+/h_\times$ polarizations

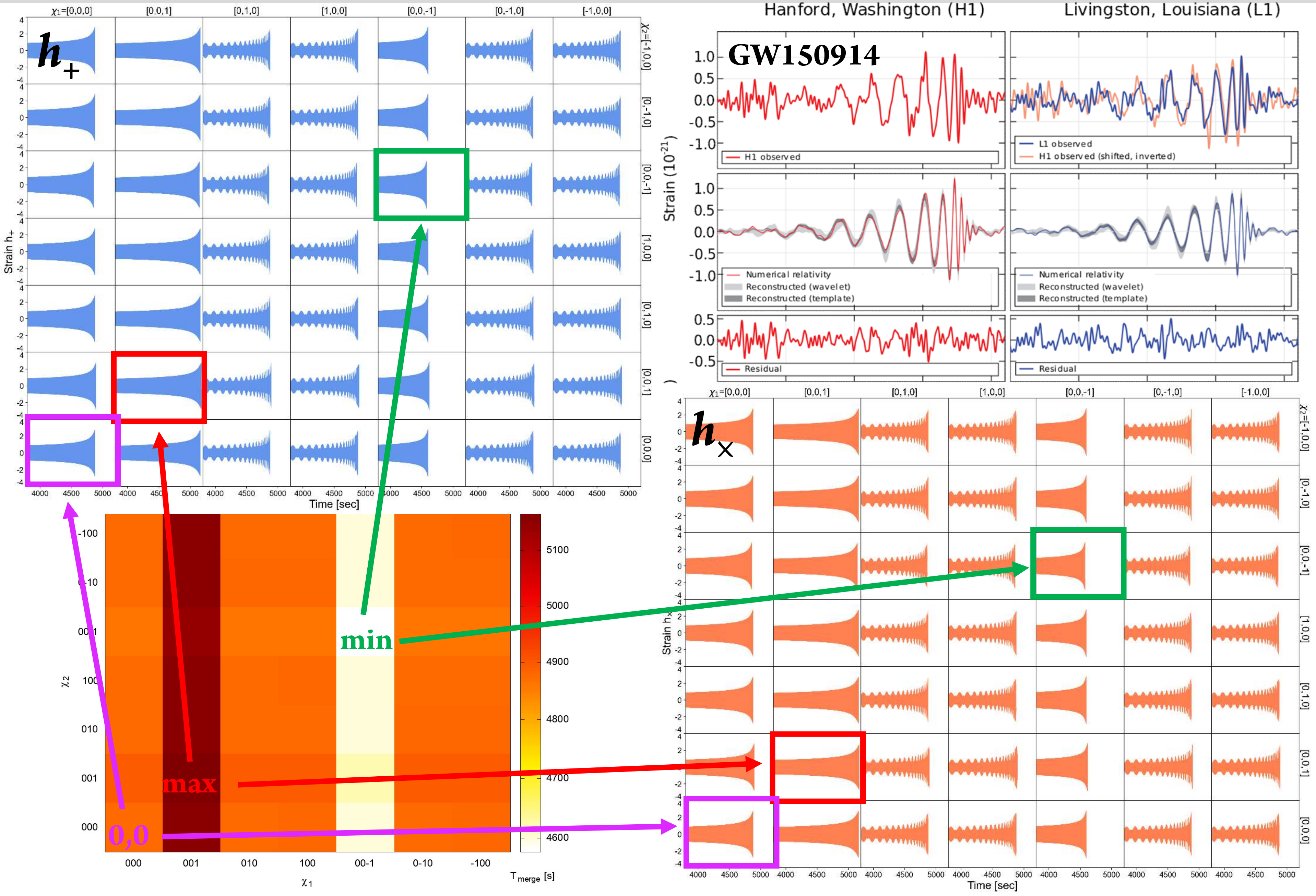

SI: Waveforms for $h_+/h_\times$ polarizations

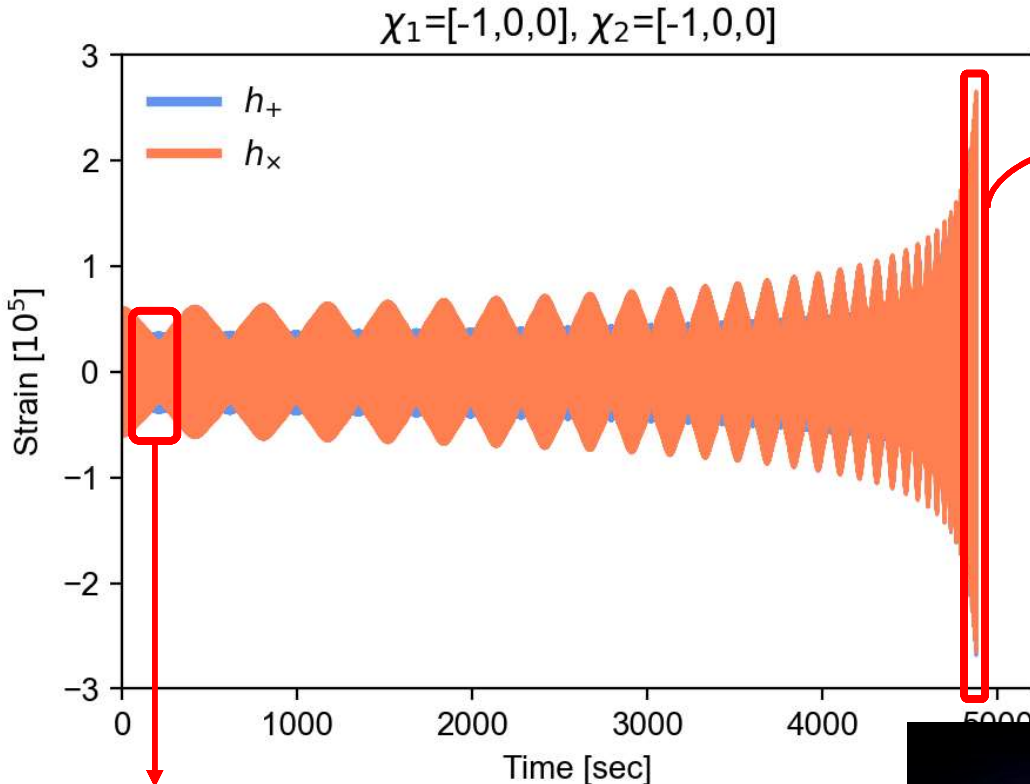

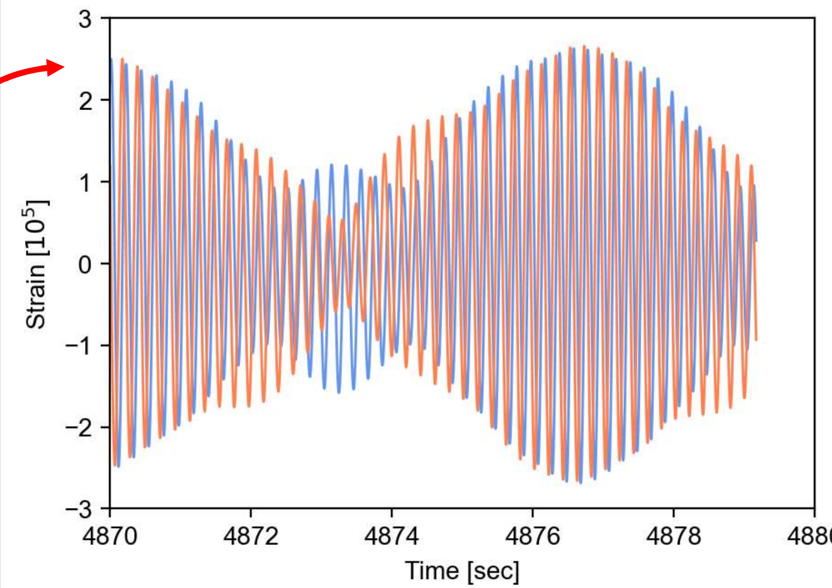

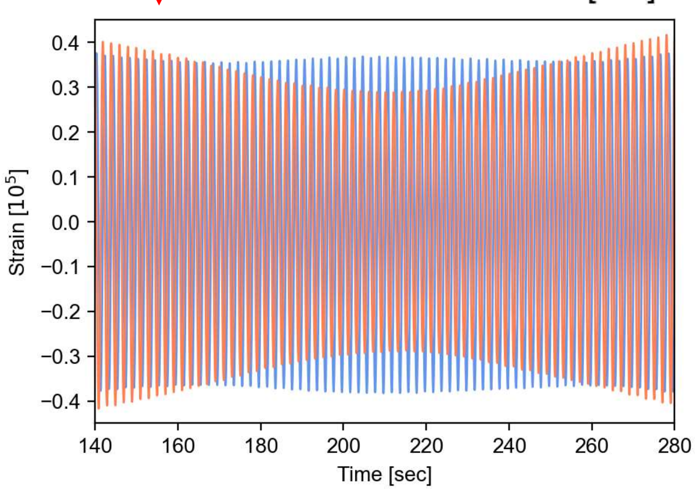

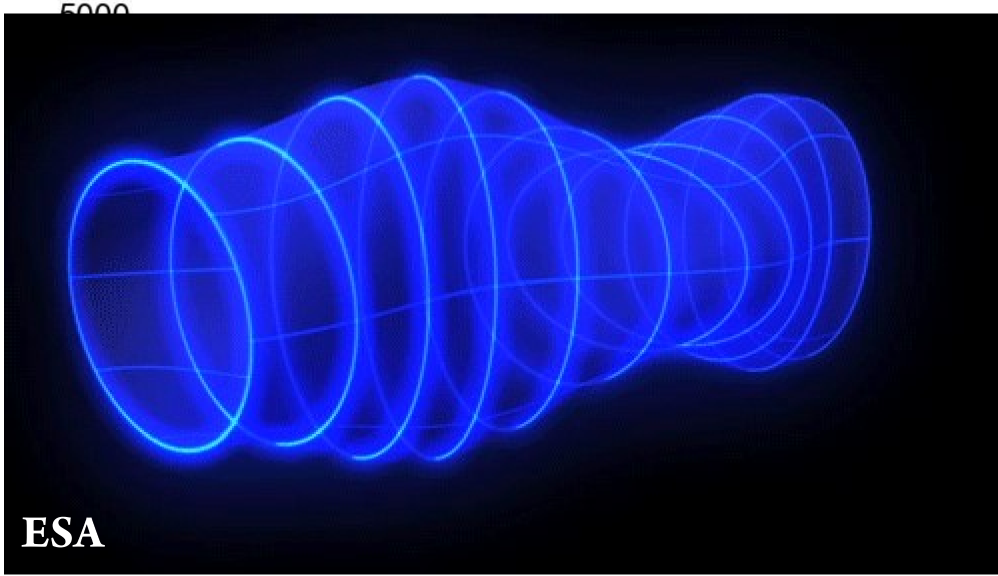

SI: Time frequency maps and $h_+/h_\times$ waveforms

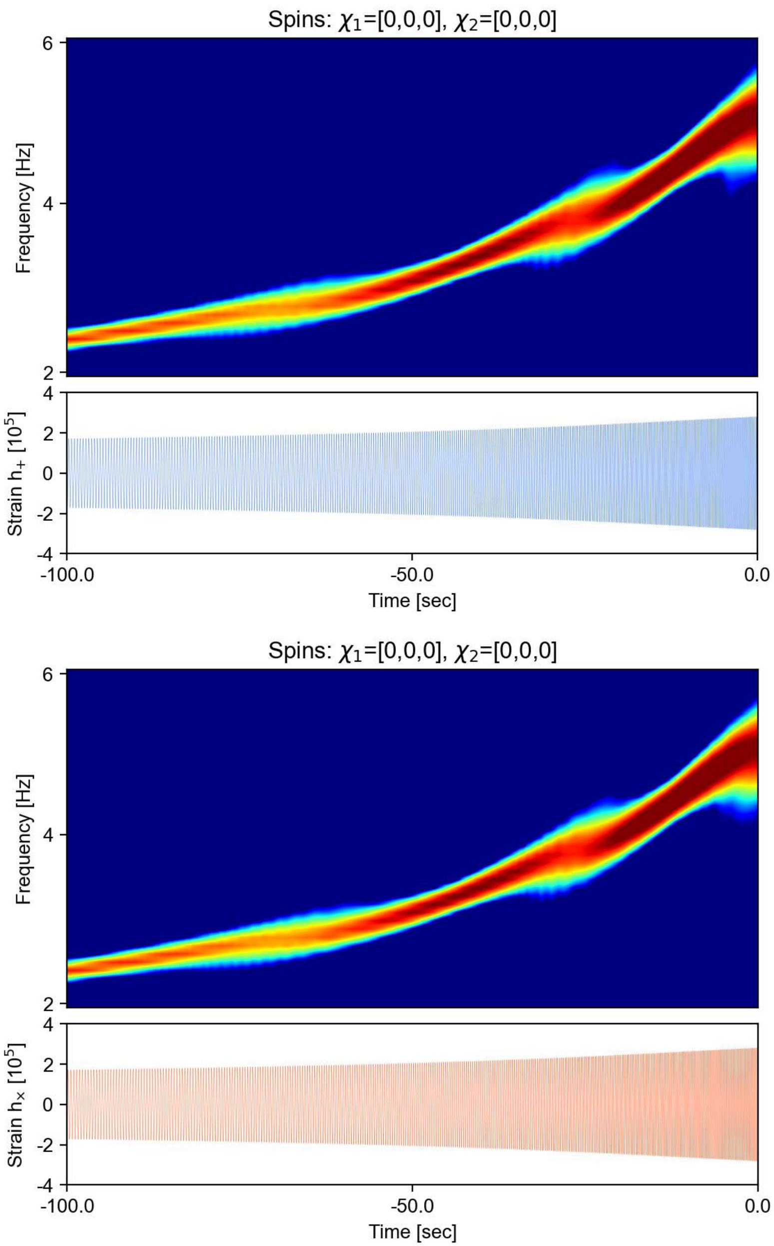

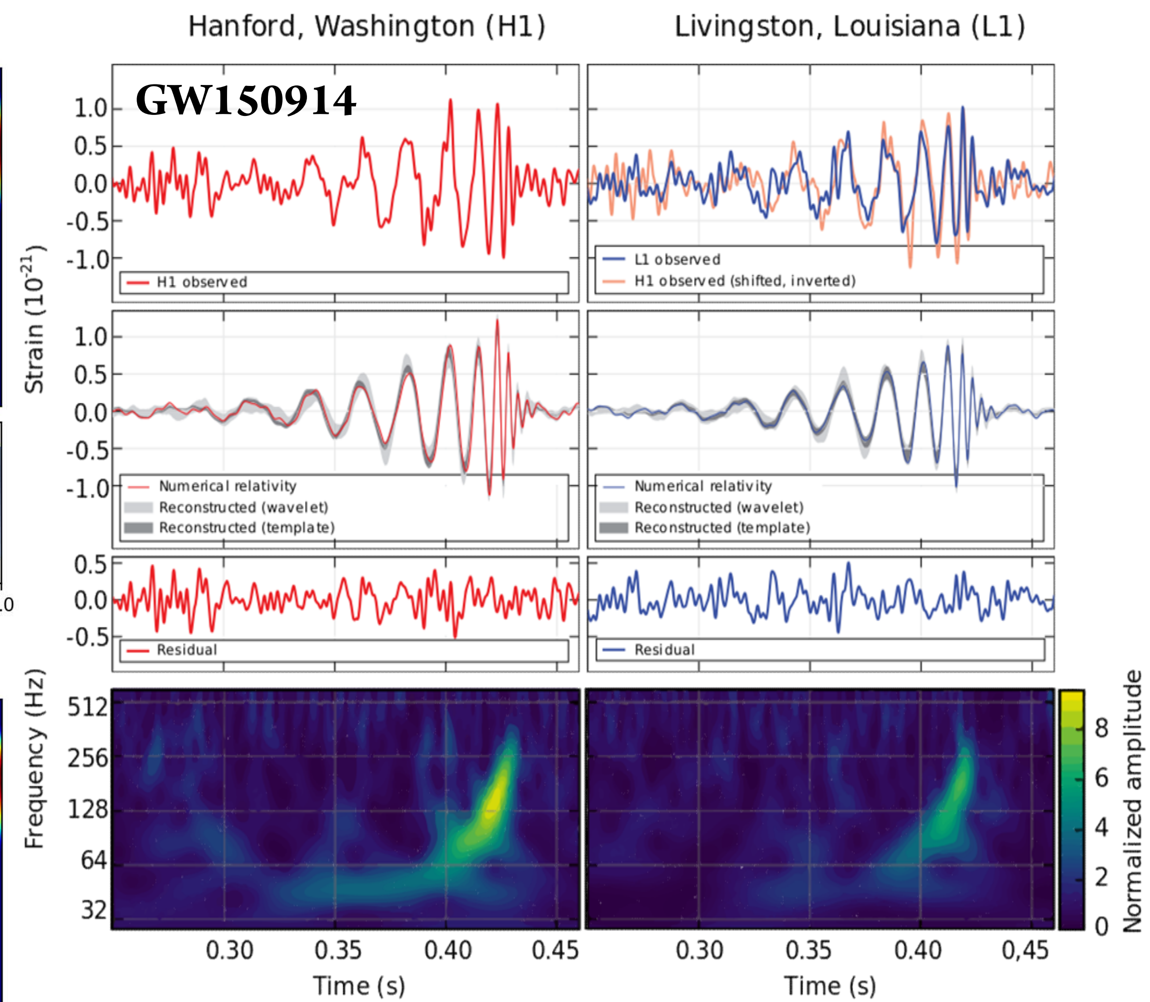

M_1=35.6 $M_\odot$, M_2=30.6 $M_\odot$, χ_{eff}=-0.01

M_1=328 $M_\odot$, M_2=21 $M_\odot$, χ_{eff}=0.0

SI: Time frequency maps and $h_+/h_\times$ waveforms

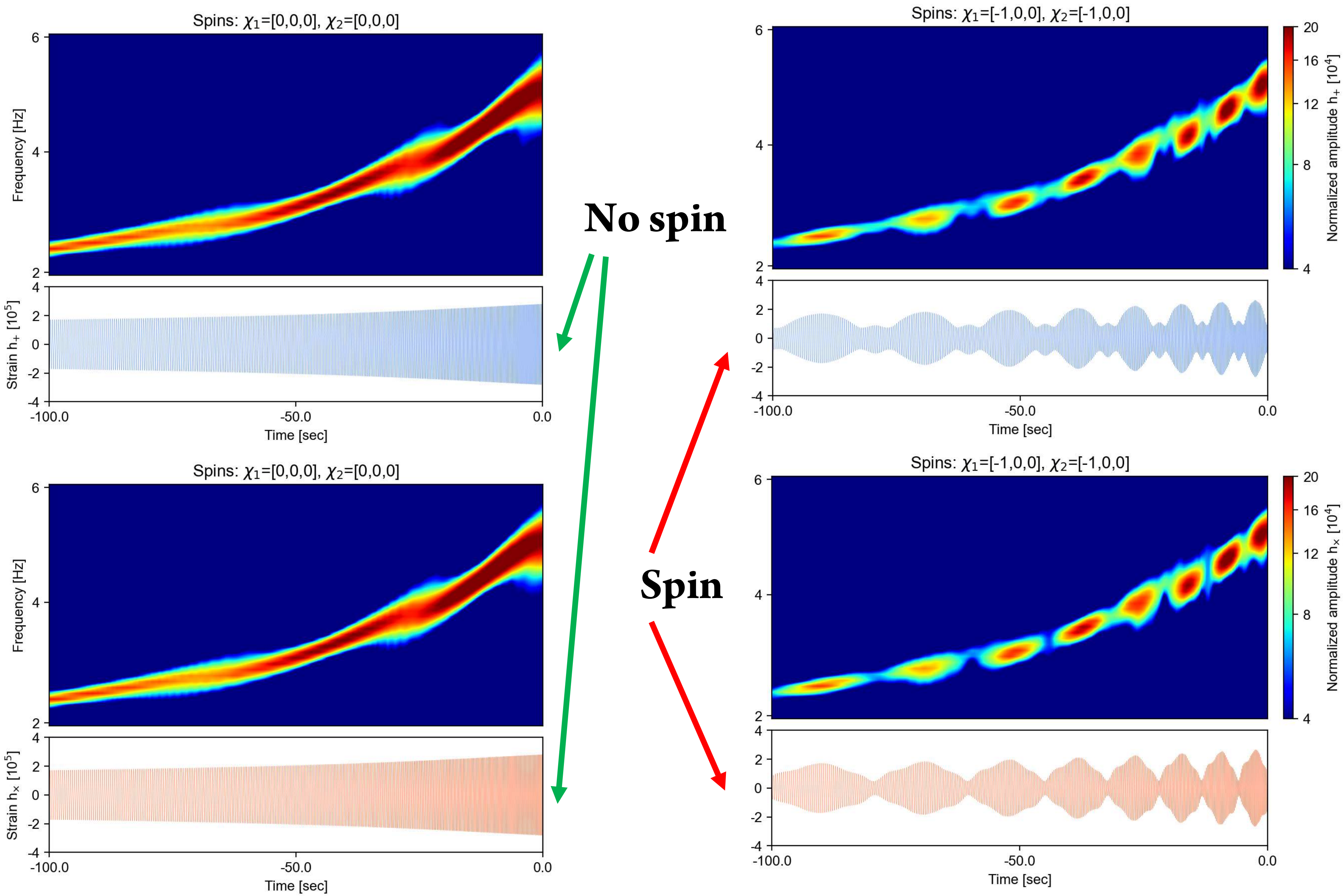

SI: Time frequency maps and h_+ waveforms

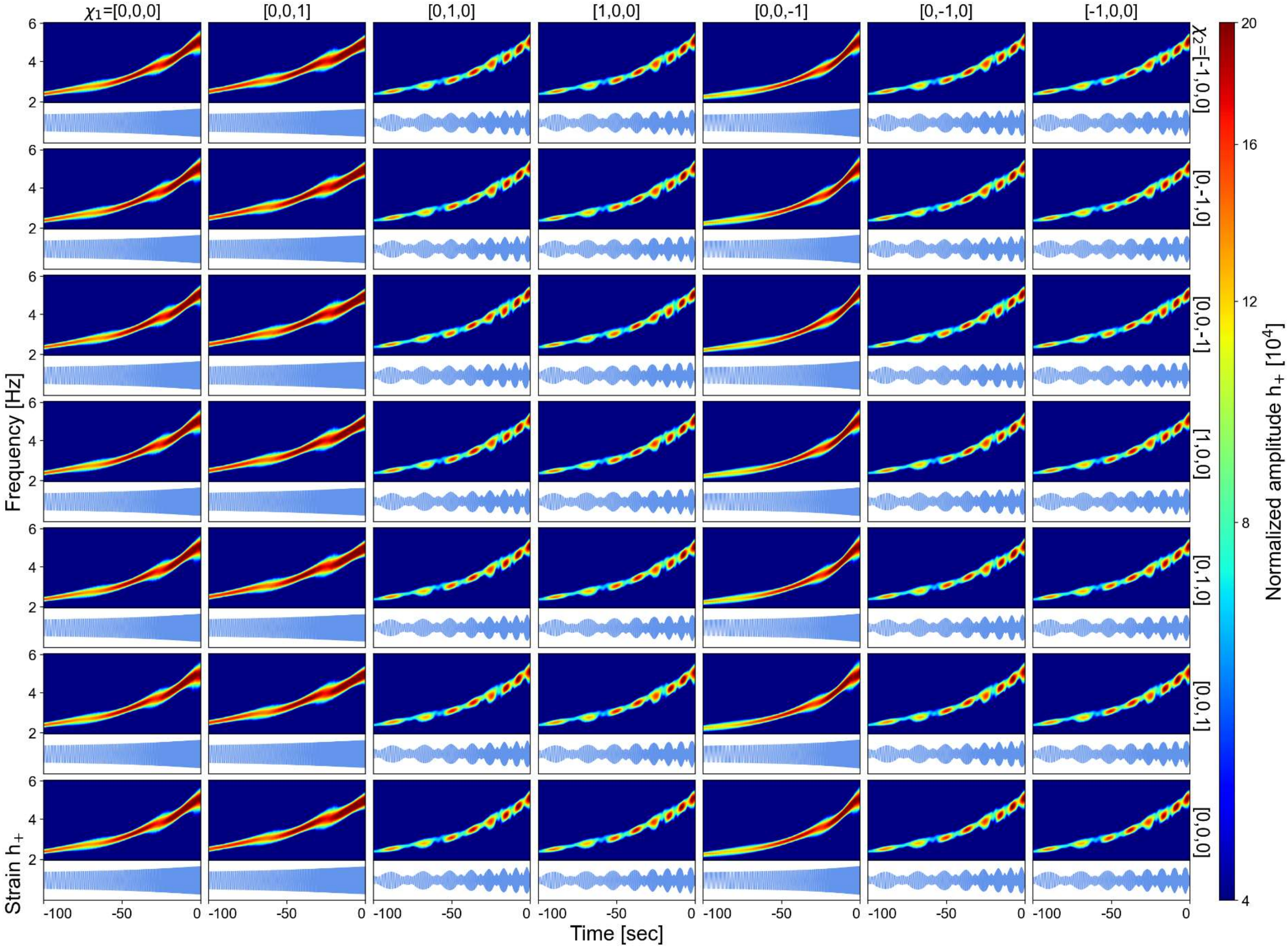

SI: Time frequency maps and $h_\times$ waveforms

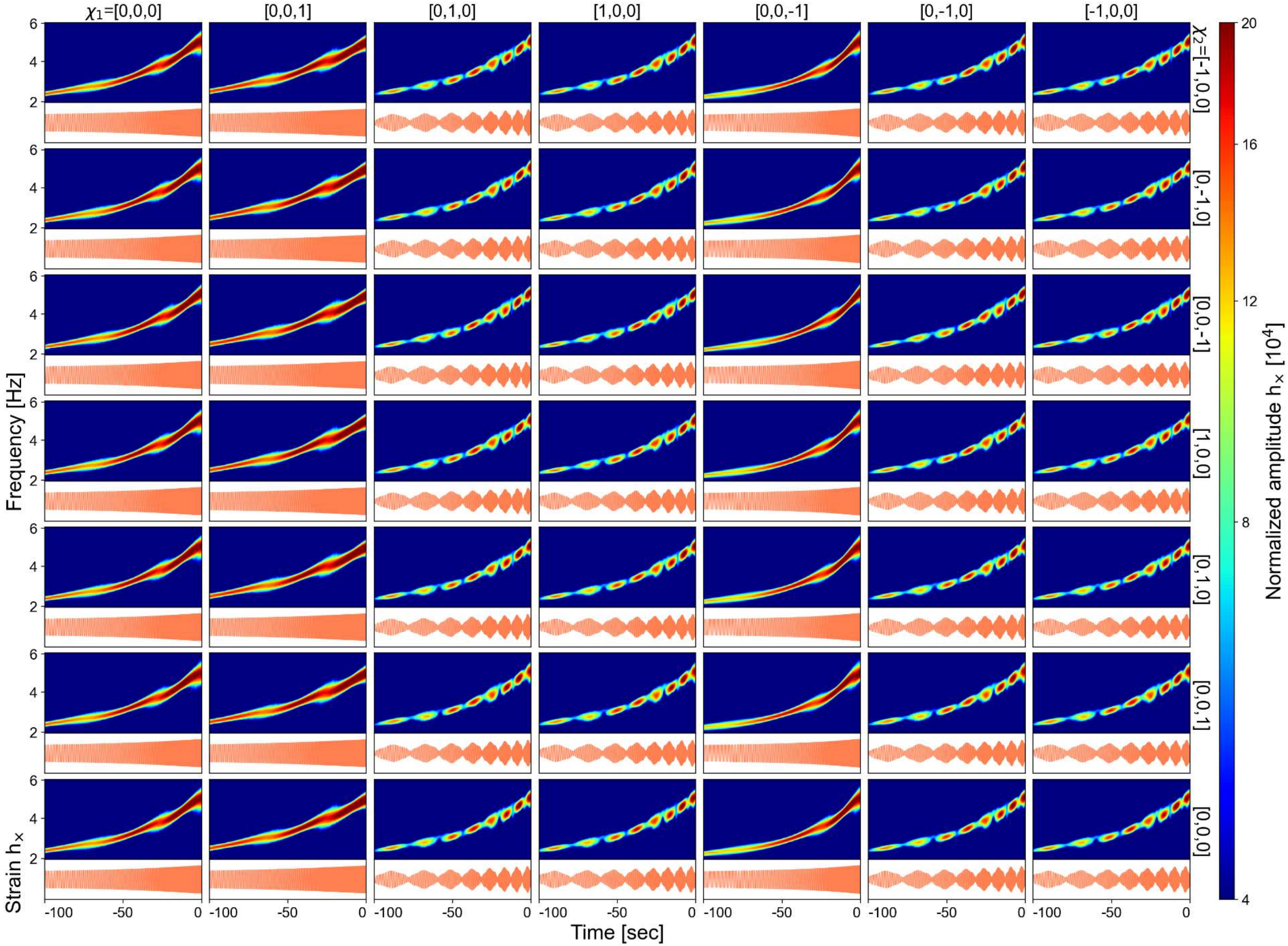

Orbit evolution

Hang up effect (***Campanelli et al., 2006PhRvD, 74, 041501***)

Up-up No-spin Antialigned spin Down-down

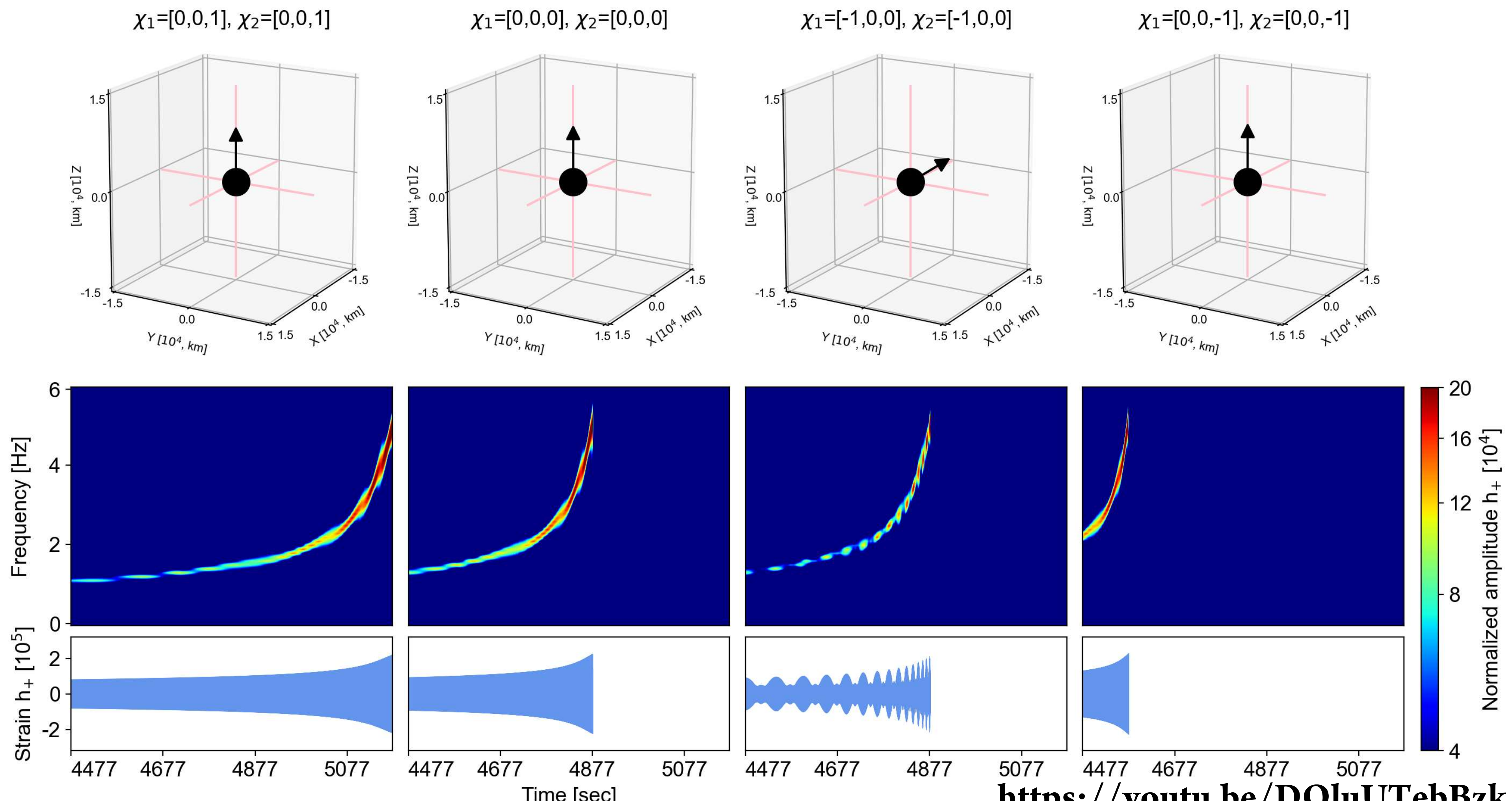

https://youtu.be/DOluUTebBzk

Orbit evolution: last 100 sec

Up-up

$\chi_1=[0,0,1]$

$\chi_2=[0,0,1]$

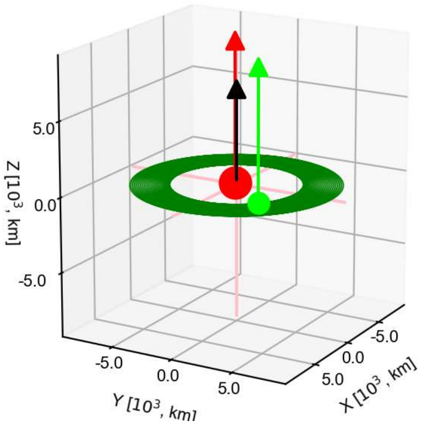

No-spin

$\chi_1=[0,0,0]$

$\chi_2=[0,0,0]$

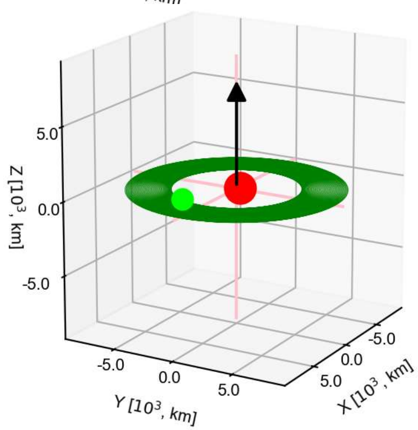

Down-down

$\chi_1=[0,0,-1]$

$\chi_2=[0,0,-1]$

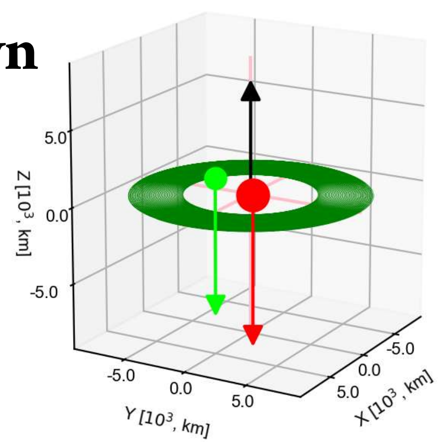

Antialigned spin

$\chi_1=[-1,0,0]$, $\chi_2=[-1,0,0]$

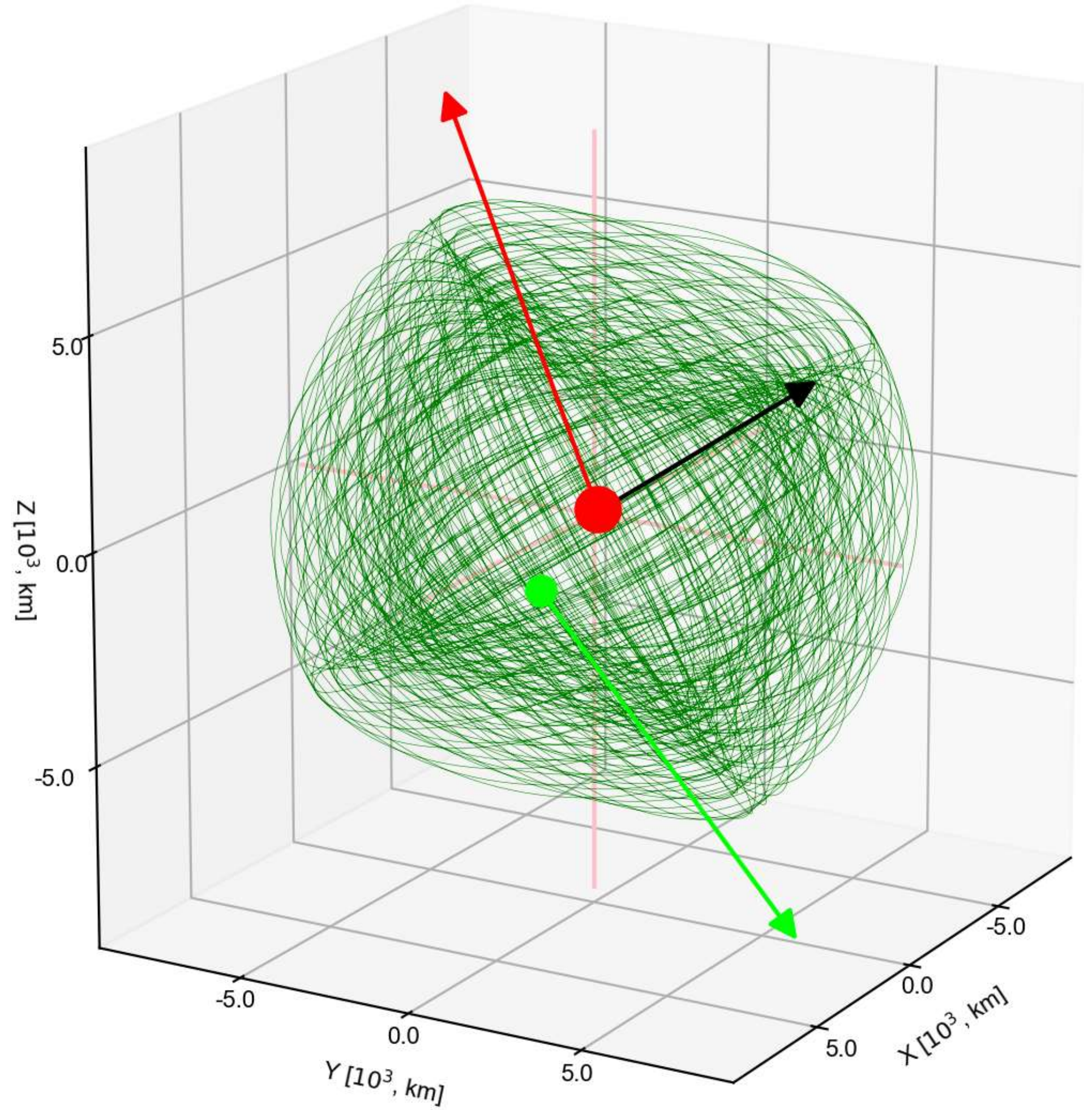

Orbit evolution: last 100 sec

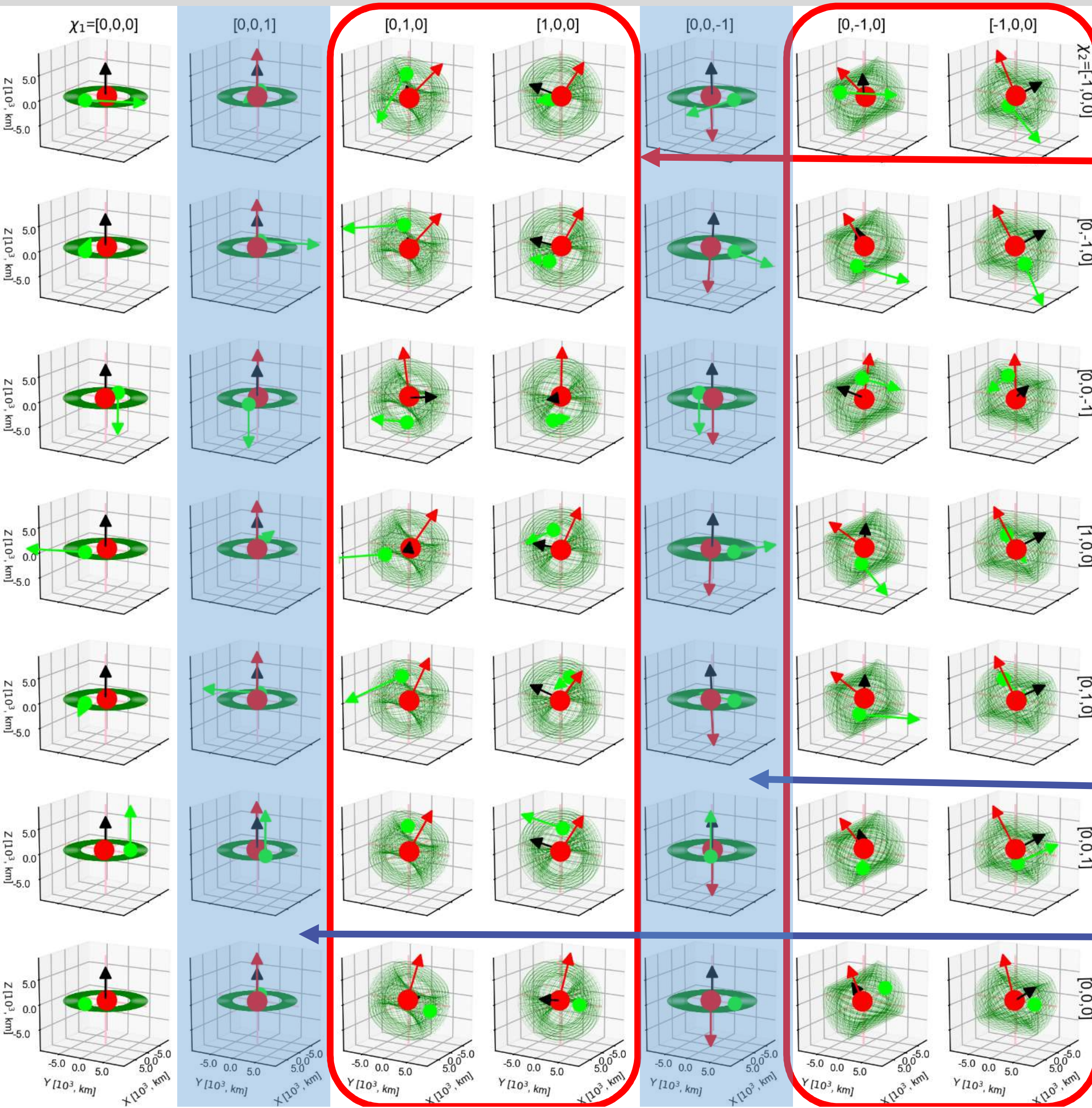

h_+

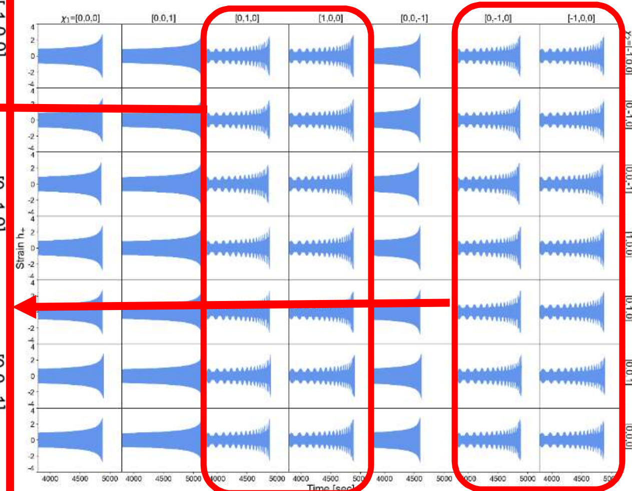

$$\chi_{eff} = \frac{m_1\chi_1 \cos\theta_1 + m_2\chi_2 \cos\theta_2}{m_1 + m_2}$$

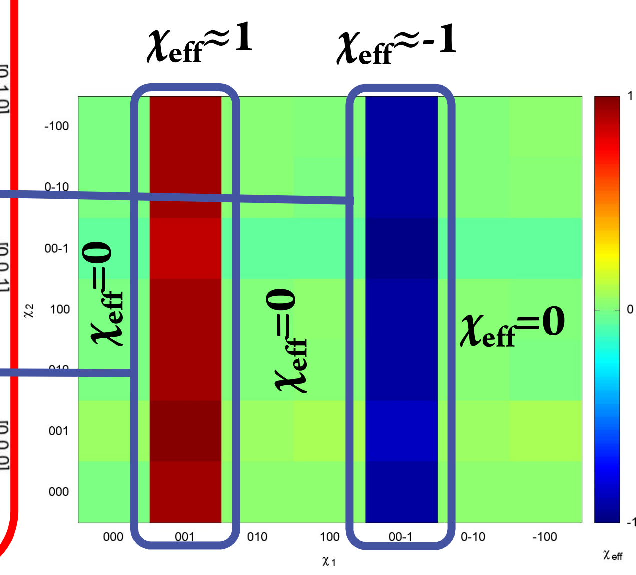

SI: Catalog of time frequency maps and $h_{+,\times}$ waveforms

M	$\mathcal{M}$	m_0	m_1	q	sma	e	t_{form}	t_{gw}	sim. up to $3.5\mathcal{P}N$
$\mathrm{M}_\odot$	$\mathrm{M}_\odot$	$\mathrm{M}_\odot$	$\mathrm{M}_\odot$		$\mathrm{R}_\odot$		Myr	yr	yr
349	62.3	328	21	0.064	1.21	0.41	113	44	69
329	62.3	307	22	0.072	0.7	0.085	348	16	16
355	70.7	329	26	0.079	697	0.997	369	3e4	4.10948e5
307	60.4	285	22	0.077	36.7	0.955	11.2	8.5e3	4.1326e4

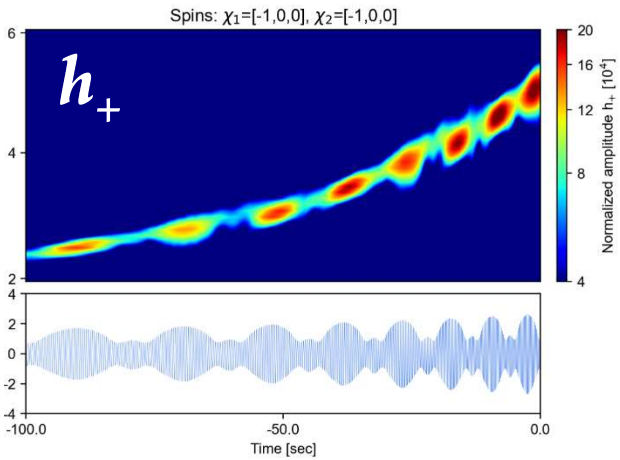

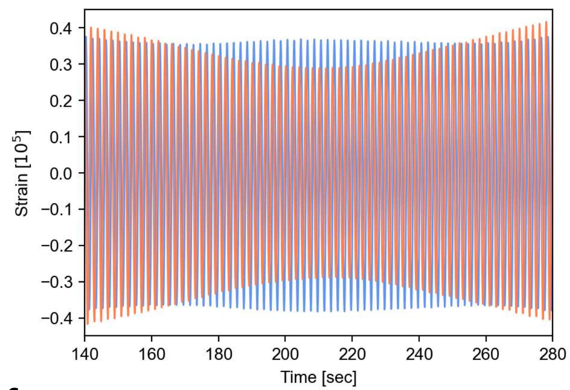

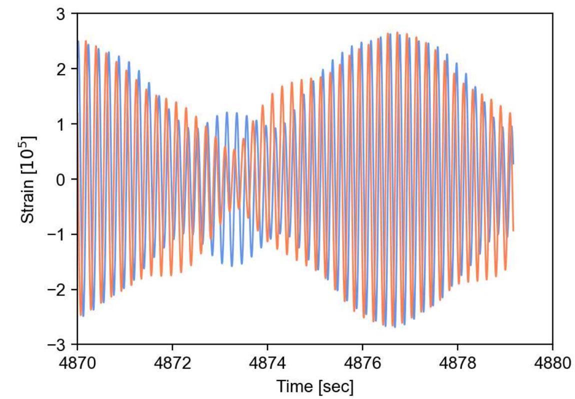

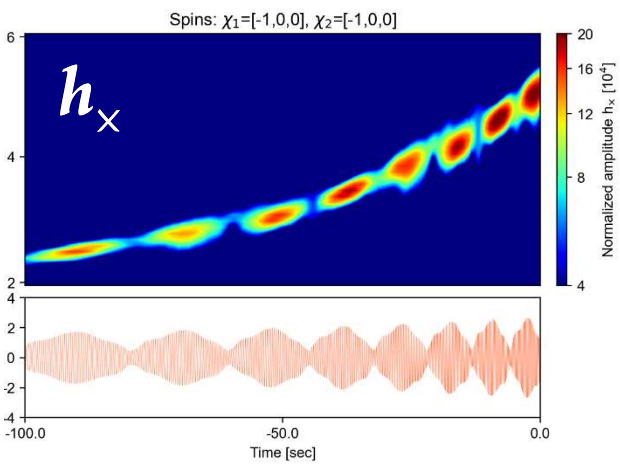

χ_{eff}		χ_0						
		000	001	010	100	00-1	0-10	-100
	-100	0.00	0.94	0.03	0.04	-0.94	0.03	0.04
	0-10	0.06	0.99	0.06	0.09	-0.88	0.06	0.09
	00-1	0.00	0.94	0.01	0.02	-0.94	0.02	-0.00
χ_1	100	0.00	0.93	0.01	0.03	-0.93	0.02	0.01
	010	-0.06	0.88	-0.06	-0.06	-0.99	-0.06	-0.06
	001	0.00	0.94	0.02	-0.00	-0.94	0.01	0.02
	000	0.00	0.93	0.02	0.01	-0.93	0.01	0.03

Properties of IMBHs escaping from star clusters

author: Konrad Maliszewski
supervisors: Mirosław Giersz, Dorota Rosińska
co-workers: Arkadiusz Hypki

18 May 2021, Teeminar

mass_buildup_mergers.txt: list of 131 binaries

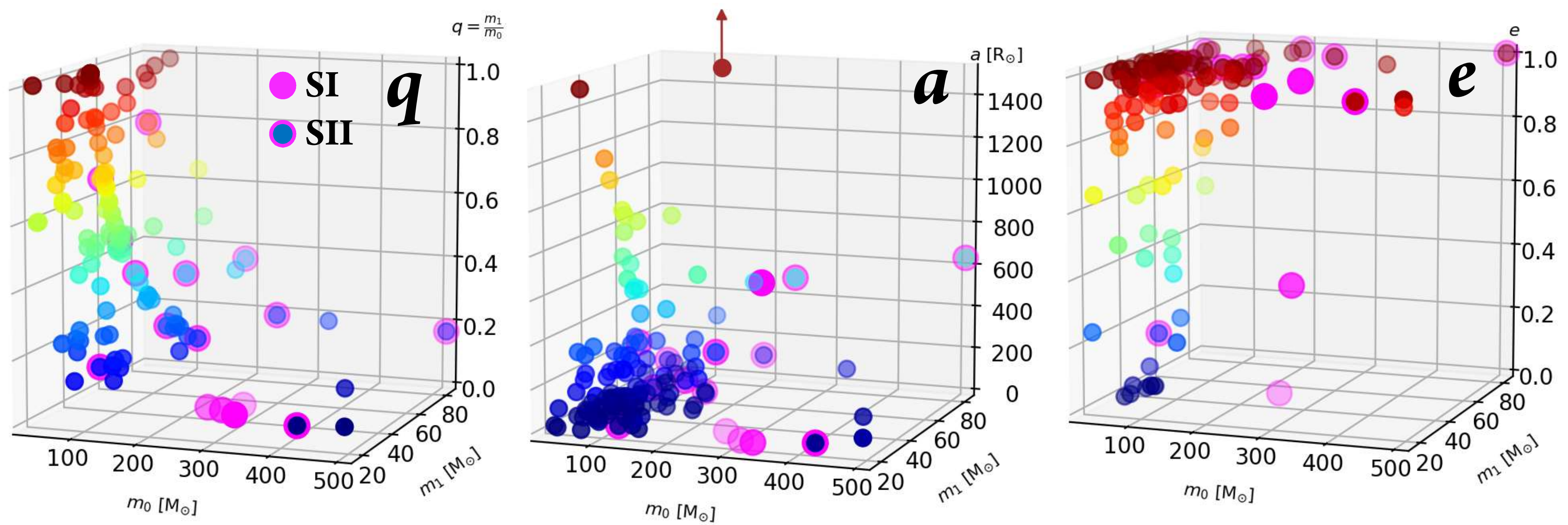

Set of models II (SII)

Run	M, $M_\odot$	$\mathcal{M}$, $M_\odot$	m_0, $M_\odot$	m_1, $M_\odot$	q	a, $R_\odot$	a, AU	e	$T_{\rm merg}$, yr	$T_{\rm merg}$, yr RK4[a]	$T_{\rm merg}$, yr sim. up to $3.5\mathcal{PN}$
2	443.181	68.2	422.6400	20.5410	0.0486016	25.0410	0.1164520	0.9559200	3.638860000E+08	3.695516913E+03	3.7787E+03
6	595.418	168.9	510.3500	85.0680	0.1666860	633.5100	2.9461200	0.9991400	8.222370000E+08	7.272909814E+02	3.340E+02
9	143.036	41.4	121.8000	21.2360	0.1743510	24.7450	0.1150760	0.9745300	9.976830000E+08	5.946445586E+03	6.2124E+03
15	256.010	79.9	211.4600	44.5500	0.2106780	284.3800	1.3225000	0.9980000	2.576190000E+08	2.813705859E+03	2.7372E+03
18	349.159	113.7	282.6700	66.4890	0.2352180	562.5900	2.6163100	0.9988600	1.990980000E+08	2.507096619E+03	2.1929E+03
25	211.460	70.4	169.2300	42.2300	0.2495420	152.0200	0.7069640	0.9952000	2.277190000E+08	7.241488106E+03	7.3900E+03
38	216.321	81.6	157.9800	58.3410	0.3692940	28.3510	0.1318450	0.9700000	8.898320000E+07	3.282037855E+03	3.3422E+03
40	282.672	107.2	205.3100	77.3620	0.3768060	133.5300	0.6209770	0.9986400	1.104350000E+08	6.988853977E+01	1.85E+01
42	157.778	60.7	112.9400	44.8380	0.3970070	95.7140	0.4451150	0.9985100	3.692100000E+08	8.508170059E+01	3.78E+01
52	134.505	54.4	89.9550	44.5500	0.4952480	303.4000	1.4109500	0.9994900	3.915930000E+08	4.317333595E+02	1.375E+02
86	106.500	45.4	63.2700	43.2300	0.6832620	0.4666	0.0021699	0.1698200	2.763830000E+08	2.208072706E+01	2.21E+01
102	144.994	62.7	79.7830	65.2110	0.8173550	132.9000	0.6180470	0.9989100	1.421000000E+08	1.257093380E+02	5.05E+01

12 (3 long runs with reduced $\Delta t_{\rm out}$) + 12*49 spin runs = **600 models**

SII

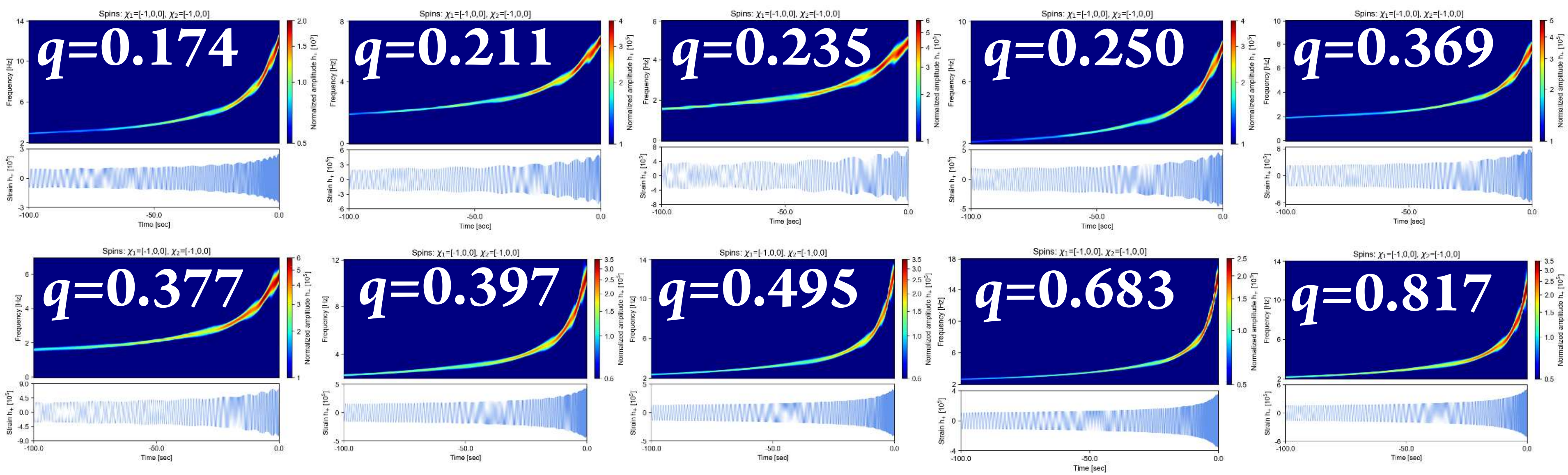

SI/SII: mass ratio q dependence

SII

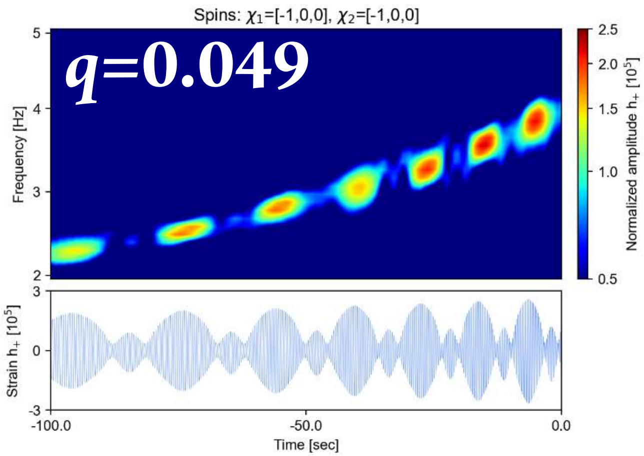

SI

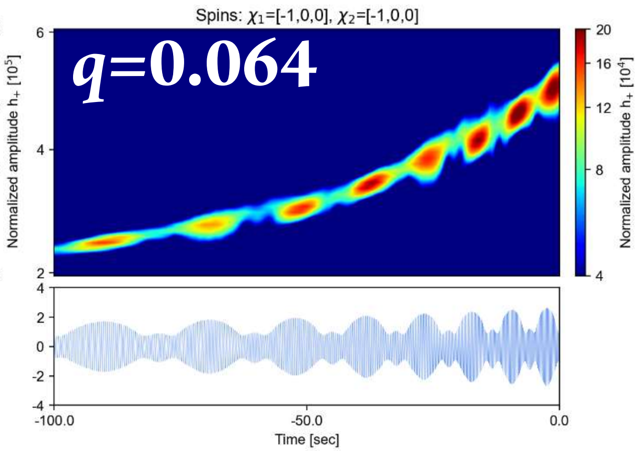

SII

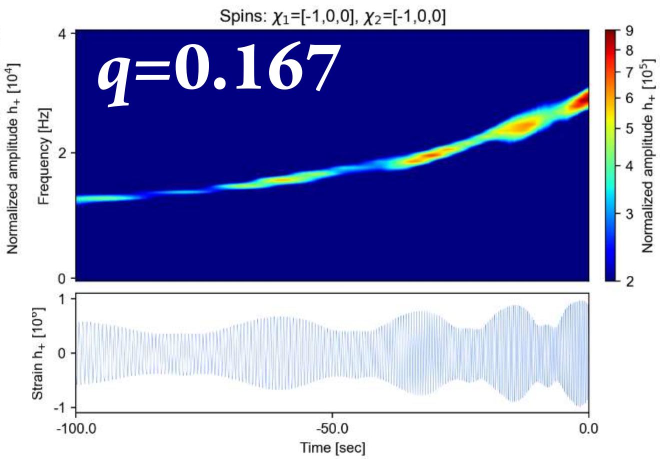

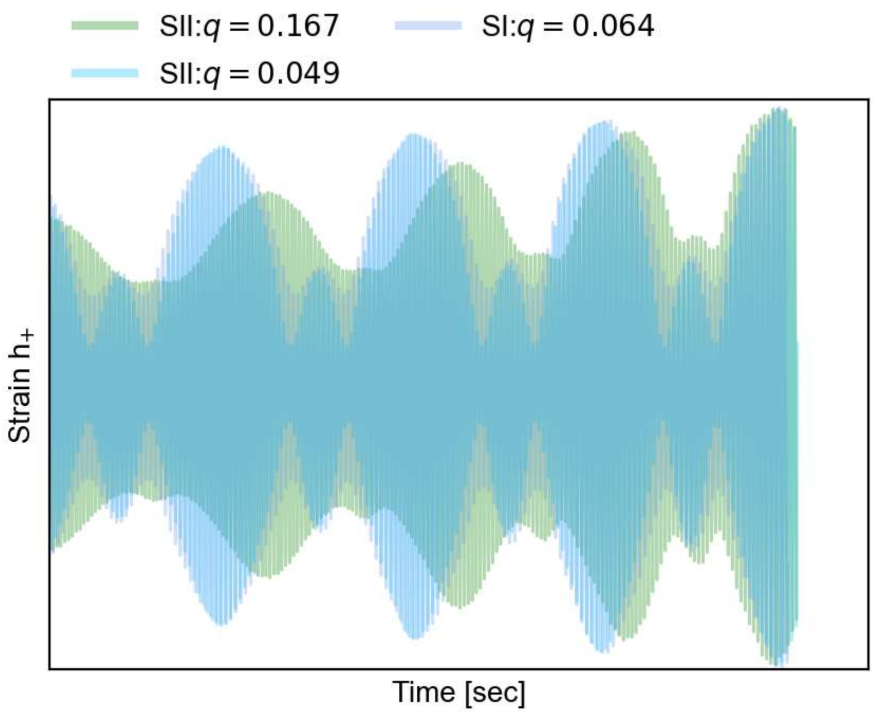

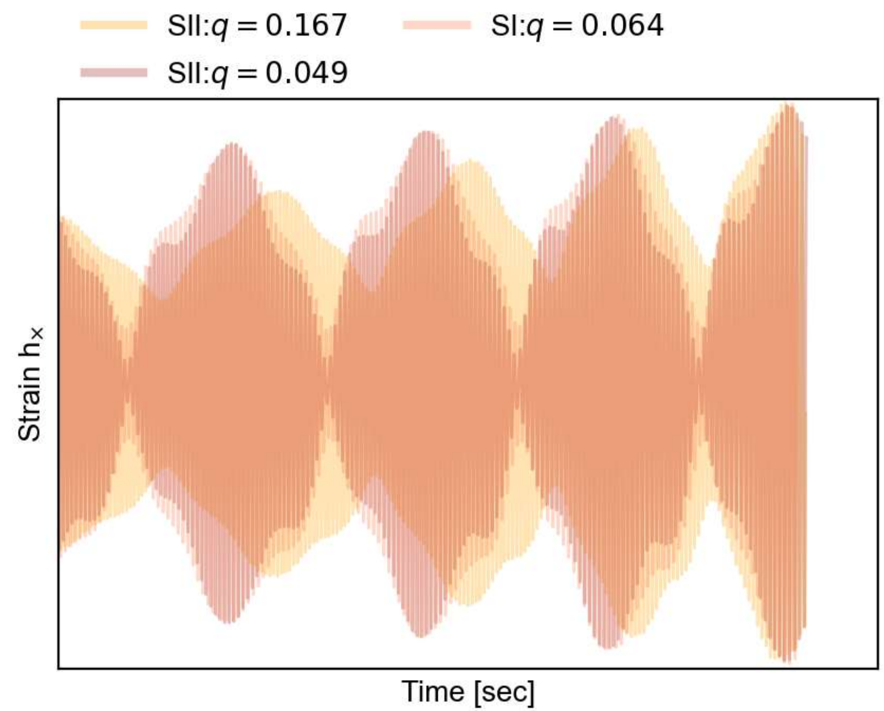

GWTC-1,2,2.1/SI/SII

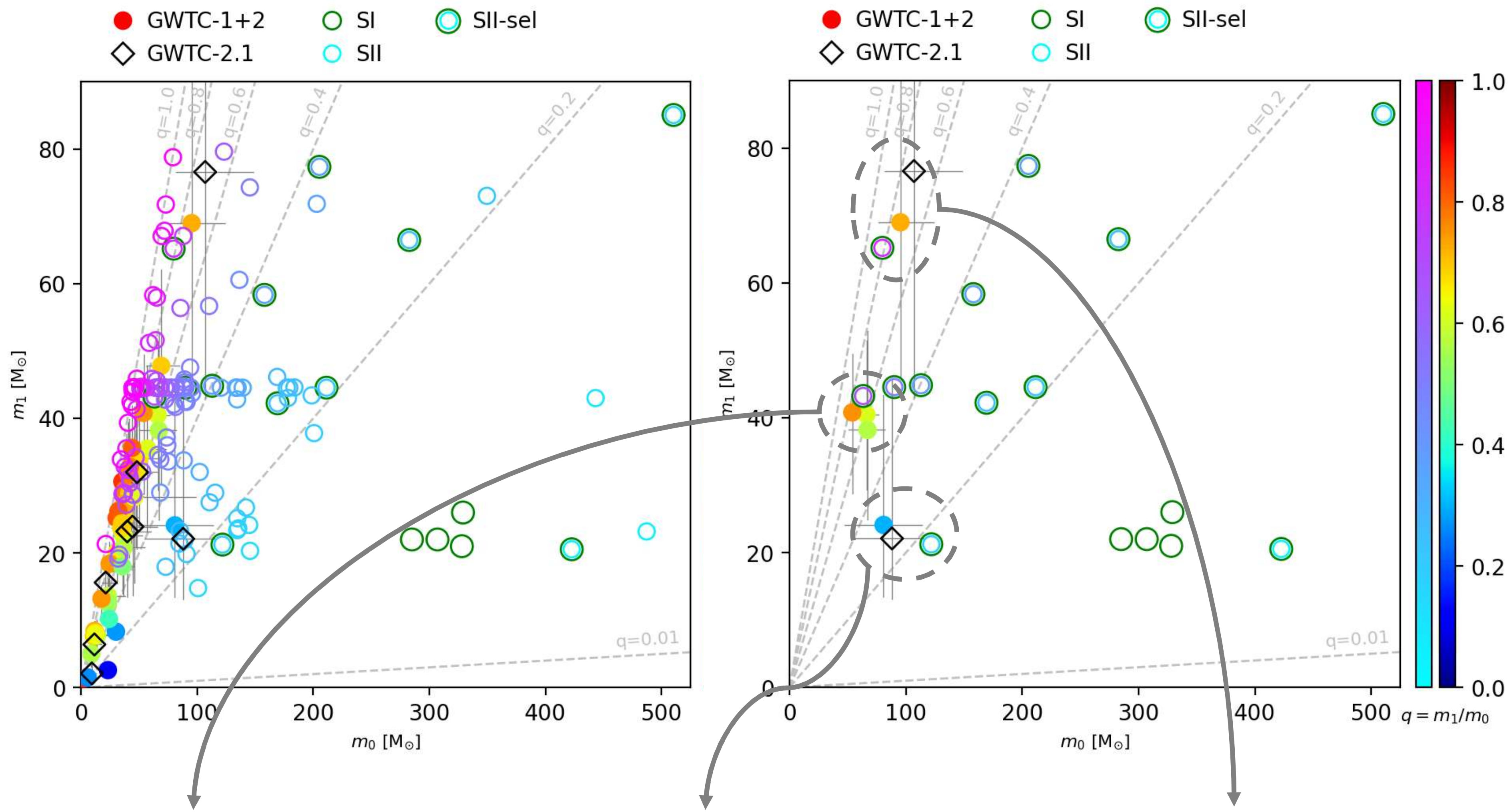

GW190519_153544
GW190701_203306
GW190706_222641
SII: 86

GW190929_012149
GW190403_051519
SII:9

GW190521
GW190426_190642
SII:102

GWTC-1,2,2.1/SI/SII

Name	M $M_\odot$	$\mathcal{M}$ $M_\odot$	m_1 $M_\odot$	m_2 $M_\odot$	q	$\chi_{\rm eff}$	comments
9	143.036	41.4	121.8000	21.2360	0.1743510		
GW190929_012149	$104.3^{+34.9}_{-25.2}$	$35.8^{+14.9}_{-8.2}$	$80.8^{+33.0}_{-33.2}$	$24.1^{+19.3}_{-10.6}$	$0.298^{+0.180}_{-0.613}$	$0.01^{+0.34}_{-0.33}$	
GW190403_051519	$110.5^{+30.6}_{-24.2}$	$36.3^{+14.4}_{-8.8}$	$88.0^{+28.2}_{-32.9}$	$22.1^{+23.8}_{-9.0}$	$0.251^{+0.138}_{-0.582}$	$0.70^{+0.15}_{-0.27}$	The primary components fall in the mass gap predicted by pair-instability supernova theory. Binary with significantly asymmetric mass ratios $q < 0.61$ at 90% credibility. Recovering a non-zero $\chi_{\rm eff}$ at 90% credibility. Primary dimensionless spin is measured to be $\chi_1 = 0.92^{+0:07}_{-0.22}$. This represents the most nearly-extremal spin observed using GWs.
86	106.500	45.4	63.2700	43.2300	0.6832620		
GW190519_153544	$106.6^{+13.5}_{-14.8}$	$44.5^{+6.4}_{-7.1}$	$66.0^{+10.7}_{-12.0}$	$40.5^{+11.0}_{-11.1}$	$0.614^{+0.230}_{-0.340}$	$0.31^{+0.20}_{-0.22}$	Source with $\chi_{\rm eff} > 0$.
GW190701_203306	$94.3^{+12.1}_{-9.5}$	$40.3^{+5.4}_{-4.9}$	$53.9^{+11.8}_{-8.0}$	$40.8^{+8.7}_{-12.0}$	$0.757^{+0.319}_{-0.321}$	$-0.07^{+0.23}_{-0.29}$	
GW190706_222641	$104.1^{+20.2}_{-13.9}$	$42.7^{+10.0}_{-7.0}$	$67.0^{+14.6}_{-16.2}$	$38.2^{+14.6}_{-13.3}$	$0.570^{+0.265}_{-0.469}$	$0.28^{+0.26}_{-0.29}$	Source with $\chi_{\rm eff} > 0$.
102	144.994	62.7	79.7830	65.2110	0.8173550		
GW190521	$163.9^{+39.2}_{-23.5}$	$69.2^{+17.0}_{-10.6}$	$95.3^{+28.7}_{-18.9}$	$69.0^{+22.7}_{-23.1}$	$0.724^{+0.354}_{-0.476}$	$0.03^{+0.32}_{-0.39}$	Previous most massive BBH. Dimensionless spin magnitude $\chi_{i=\{1,2\}} > 0.8$ with 58% credibility.
GW190426_190642	$184.4^{+41.7}_{-36.6}$	$77.1^{+19.4}_{-17.1}$	$106.9^{+41.6}_{-25.2}$	$76.6^{+26.2}_{-33.6}$	$0.717^{+0.427}_{-0.542}$	$0.19^{+0.43}_{-0.40}$	The primary components fall in the mass gap predicted by pair-instability supernova theory. Supersedes the previous most massive BBH.

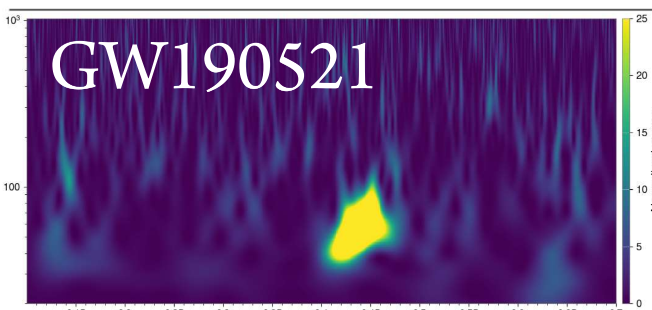

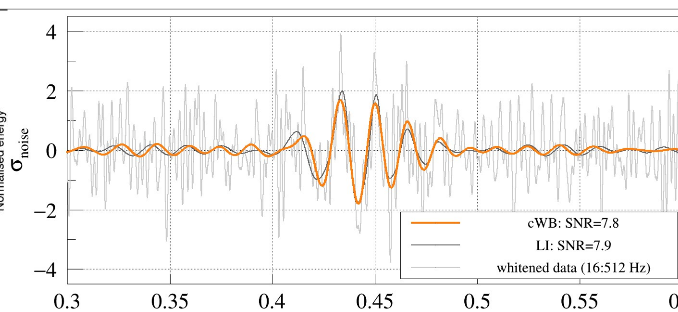

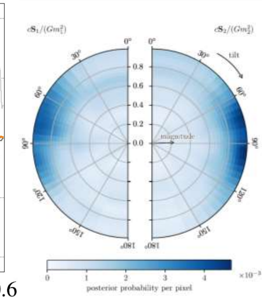

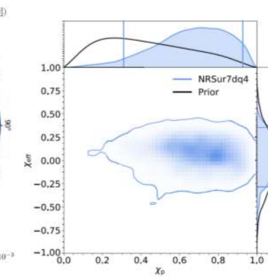

GWTC-1,2,2.1/SI/SII

$$m_0 = 13.7^{+8.8}_{-3.2}$$
$$m_1 = 7.7^{+2.2}_{-2.5}$$
$$\chi_{\rm eff} = 0.18^{+0.20}_{-0.12}$$

GW151226 - Hanford

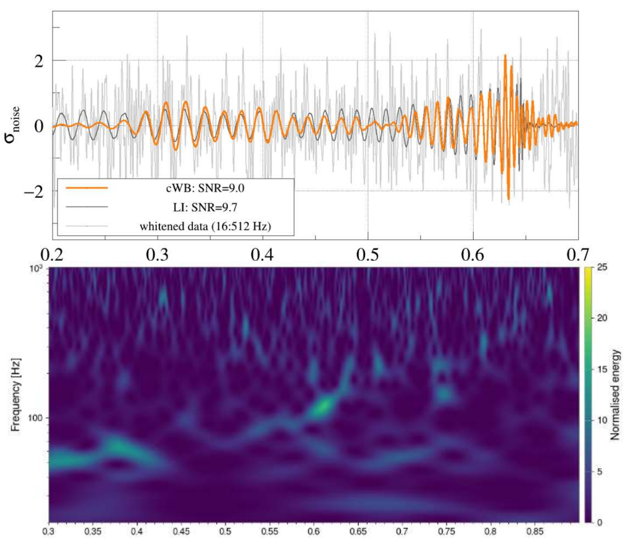

$$m_0 = 11.0^{+5.5}_{-1.7}$$
$$m_1 = 7.6^{+1.4}_{-2.2}$$
$$\chi_{\rm eff} = 0.03^{+0.19}_{-0.07}$$

GW170608 - Hanford

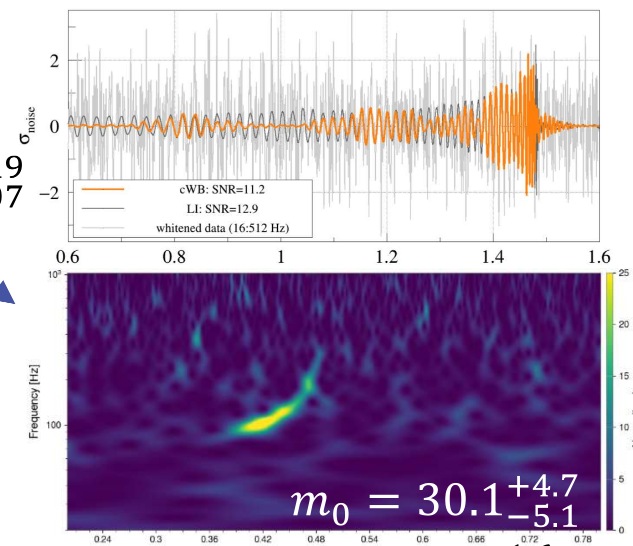

$$m_0 = 11.6^{+3.3}_{-1.7}$$
$$m_1 = 8.4^{+1.4}_{-1.7}$$
$$\chi_{\rm eff} = -0.05^{+0.10}_{-0.08}$$

$$m_0 = 12.3^{+7.2}_{-2.2}$$
$$m_1 = 8.1^{+1.7}_{-2.6}$$
$$\chi_{\rm eff} = 0.12^{+0.20}_{-0.07}$$

$$m_0 = 30.1^{+4.7}_{-5.1}$$
$$m_1 = 8.3^{+1.6}_{-0.9}$$
$$q = 0.28^{+0.12}_{-0.06}$$
$$\chi_{\rm eff} = 0.25^{+0.08}_{-0.11}$$

GW190707_093326 - Livingston

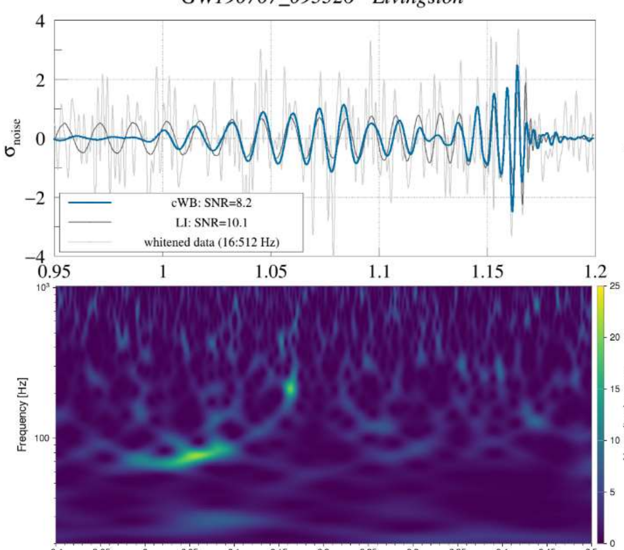

GW190728_064510 - Livingston

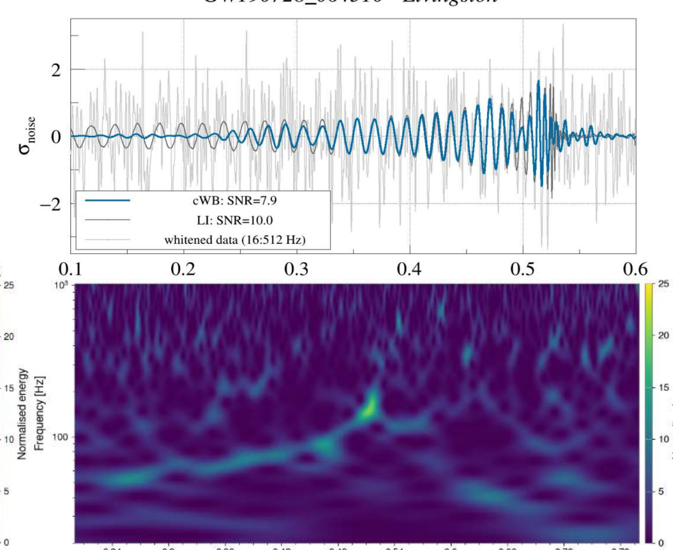

GW190412 - Livingston

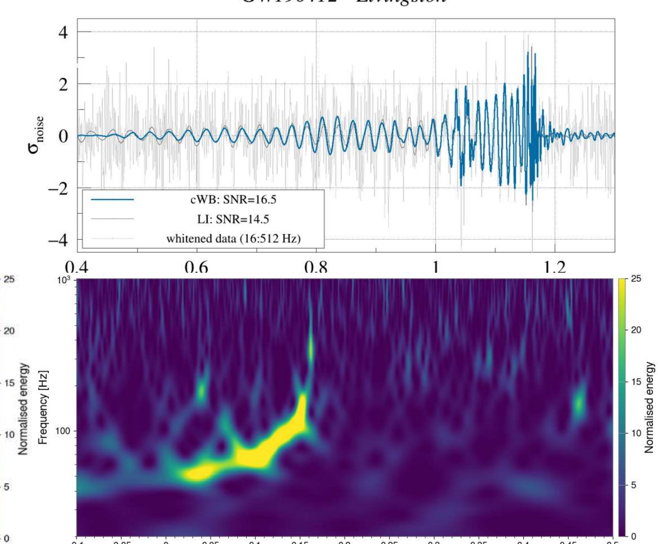

Preliminary results

- We obtained h_+ *and* $h_\times$ polarization waveforms and time frequency maps for set of BBHs with mass ratio q= 0.064-0.0817 and 49 spin combinations.
- System with beating in waveforms should have non-zero spin $\chi_{1,2}$ at least for a more massive BH and non-symmetric mass ratio q.
- System with non-zero effective spin χ_{eff} should have non-zero spin $\chi_{1,2}$ at least for a more massive BH. If such systems have non-symmetric mass-ratio q we should see beating in waveforms and time-frequency picture .

To do list

- Move from h_+ *and* $h_\times$ polarization waveforms to some linear combination $h(t)$, which detected by LIGO-Virgo-KAGRA.
- Estimate precessing spin parameter χ_{p}.
- Estimate final mass M_{f} and final spin χ_{f} after merging.
- Continue simulations with numerical relativity, effective one body etc... ?

Caveats

- Waveforms and time–frequency maps obtained just for early inspiral, not late inspiral and merging, because we work with PN terms.
- In our models we use maximum value of spin and chosen directions, which do not cover the full space of parameters.

WORK IN PROGRESS

Deborah Ferguson, Karan Jani, Deirdre Shoemaker, Pabla Laguna